

Non-parametric IQC Multipliers in Data-Driven Robust Controller Synthesis

Vaibhav Gupta, Elias Klauser, and Alireza Karimi

Abstract—The paper presents a robust data-driven controller synthesis method for generalised multi-input multi-output (MIMO) systems. Using the frequency response of a linear time-invariant (LTI) MIMO system and characterising perturbations through Integral Quadratic Constraint (IQC), the method provides a convex set of controllers robust to perturbations. This facilitates the design of controllers with either robust stability or robust performance criteria. Notably, the proposed method is versatile, as it is also applicable for non-parametric IQC multipliers. An example of a non-parametric IQC multiplier for elliptical uncertainty quantification is demonstrated and subsequently employed in designing a robust controller for a hybrid active-passive micro-vibration platform. Experimental results show that the synthesised controller effectively achieves the desired levels of both robustness and performance.

Index Terms—Robust control; uncertain systems; Optimal control; LMIs

I. INTRODUCTION

INTEGRAL Quadratic Constraints (IQC) offer a versatile and flexible formalism for representing and analysing a wide range of uncertainties and nonlinearities including parametric uncertainties, rate-bounded uncertainties, time-delay uncertainties, as well as norm- and sector-bounded nonlinearities. In [1], a sufficient condition for robust closed-loop stability in systems with IQC-type uncertainties/nonlinearities is described. Various extensions to the IQC framework, incorporating aspects of dissipation theory [2], [3], as well as elements of Lyapunov theory [4] has been introduced in the literature. The IQC approach has been shown to be linked to various stability notions, including classical multiplier theory [5] and graph separation theory [6]. Furthermore, within the IQC framework, a concept of system stability margin has been introduced for systems with mixed uncertainties [7]. Several techniques for analysing the robustness of the systems have been proposed. For example, [8] presents a method for a linear parameter-varying (LPV) system, while [9] offers an efficient approach for robustness analysis using the IQC framework.

While the majority of existing literature in IQC focuses on robustness analysis, there is also a subset of research dedicated to controller synthesis using the IQC framework.

This work is funded by the Swiss National Science Foundation under grant no. 200021-204962 and by the European Space Agency (ESA) with Contract No. 4000133258/20/NL/MH/hm.

V. Gupta and A. Karimi are with Laboratoire d'Automatique, École Polytechnique Fédérale de Lausanne (EPFL), Switzerland (e-mail: vaibhav.gupta@epfl.ch, alireza.karimi@epfl.ch).

E. Klauser is with CSEM SA, Neuchâtel, Switzerland (e-mail: elias.klauser@csem.ch).

For instance, [10] introduced a model-based control synthesis approach, complemented by the availability of the associated MATLAB package IQClab [11]. It should be noted that the method uses an iterative procedure which alternates between nominal controller synthesis and IQC-analysis, and hence no optimality certificate can be provided. A robust synthesis method for uncertain LPV systems has been addressed in [12] that similarly alternates between the LPV synthesis step and the IQC analysis step. A novel IQC synthesis framework, which employs non-smooth optimisation for the synthesis of the structured controllers, has been recently presented in [13]. This approach addresses the issue of providing an optimality certificate but necessitates the multiplier to have a specific structure.

Due to recent developments in computational capabilities and sensing technologies, data-driven controller synthesis is emerging as a valuable alternative to the conventional model-based approaches. These data-driven approaches are particularly beneficial in scenarios where a system model is either unavailable or challenging to estimate. The utilisation of frequency response data for the analysis and synthesis of controllers in linear systems has become a well-established practice in the literature. The frequency response of the system can be easily extracted from the input-output data, as presented in [14], leading to its widespread adoption in the industry for the classical loop-shaping approaches. Considering that a substantial portion of control performance and robust stability criteria can be formulated in the frequency domain, numerous frequency domain data-driven techniques have been introduced in the literature.

In general, the controller design using frequency-domain data leads to a non-convex optimisation problem. This optimisation problem is solved using a non-smooth optimisation framework in [15] to compute fixed structure \mathcal{H}_∞ controllers for systems represented by their frequency-domain data. Several solutions have also been proposed using convex approximations. The design of SISO-PID controllers through convex optimization using frequency domain data was proposed by [16] and [17]. This approach involves employing the same type of linearization of constraints as presented in the work of [18]. The design of MIMO-PID controllers was presented by [19] as a convex-concave optimization, which is solved by linearization of quadratic matrix inequalities. In [20], a frequency-based data-driven control design methodology with an \mathcal{H}_∞ control objective based on coprime factorisation of the controller is proposed and extended to systems with sector nonlinearity [21]. This method is also employed for LPV con-

troller design in [22]. A fixed-structure data-driven controller design method for multivariable systems with mixed $\mathcal{H}_2/\mathcal{H}_\infty$ sensitivity performance is proposed in [23] and applied to the distributed control of microgrids [24] and passivity-based controller design [25]. Finally, [26] extends the technique to the fixed-structure controller design problem for generalised systems represented in linear fractional representation (LFR) form. While some techniques have been extended to account for certain nonlinearities, a comprehensive data-driven controller design framework for generalised systems that accounts for generic nonlinearities is absent.

Within the data-driven context, the existing results for controller synthesis with robust stability using IQC framework are fairly limited. Nevertheless, [27] established a necessary and sufficient condition for assessing the stability of linear time-invariant (LTI) system using only one input–output trajectory of finite length. A data-driven approach that merge robust stability with performance analysis within the IQC framework for LPV controller synthesis has been explored in [28], and deployed for control of a gyroscope [22].

This paper presents a data-driven controller synthesis for generalised MIMO systems in the presence of perturbations characterised by non-parametric IQCs. The contributions of this paper are:

- 1) Development of a convex set of robustly stabilising controllers for generalised systems in the presence of perturbations characterised by non-parametric IQC.
- 2) Robust controller synthesis method for generalised MIMO plants, using only frequency-domain measurement data, with robust stability or robust performance guarantees.
- 3) Derivation of a non-parametric IQC multiplier directly from frequency-domain data, which is employed to ensure robust stability guarantees of the synthesised controller.

The organisation of the paper is as follows: In Section II, basic notations are introduced, an overview of IQC is provided, and the context for the problem under consideration is established. The main developments of the paper are presented in Section III. In Section III-A, the convex set of controllers ensuring robust stability is presented. Furthermore, the approach is extended for robust performance by integrating a performance channel in Section III-B. A data-driven method for computing non-parametric IQC multipliers is presented in Section IV, and is employed in Section V to synthesise a robust controller for a hybrid active-passive micro-vibration damping platform, considering uncertainties in its mechanical properties.

II. PRELIMINARIES

Notations: \mathbb{R} represents the set of real numbers, while \mathbb{C} denotes the set of complex numbers. The set of real rational stable transfer functions with bounded infinity norm is denoted by \mathcal{RH}_∞ . The notation $M \succ (\succeq)$, N signifies that the matrix $M - N$ is positive (semi-) definite, and $M \prec (\preceq)$, N signifies that $M - N$ is negative (semi-) definite. The identity matrix of the appropriate size is denoted by I . The conjugate transpose

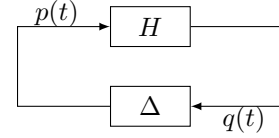


Fig. 1. Basic feedback configuration

of a complex matrix M is indicated as M^* . The conjugate transpose of the diagonally opposed element in a square matrix is denoted by \star . If $M \in \mathbb{C}^{n \times m}$ is full row rank, its right inverse is defined as $M^R = M^*(MM^*)^{-1}$. It is evident that $MM^R = I$ and $M^R M$ are Hermitian. In the case of full column rank, the left inverse is denoted as $M^L = (M^* M)^{-1} M^*$. Consequently, $M^L M = I$, and $M M^L$ is Hermitian. For a square matrix with full rank, $M^R = M^L = M^{-1}$. $\mathcal{R}(M)$ and $\text{rank}(M)$ represent the range and rank of the matrix M , respectively. A decomposition function $\mathcal{C} : \mathbb{C}^{m \times n} \mapsto \mathbb{R}^{2m \times 2n}$ and its inverse \mathcal{C}^{-1} are also defined,

$$\mathcal{C}(x) \triangleq \begin{bmatrix} \text{Re}\{x\} \\ \text{Im}\{x\} \end{bmatrix} \quad \text{and} \quad \mathcal{C}^{-1}(y) \triangleq \begin{bmatrix} I & jI \end{bmatrix} y.$$

For continuous-time systems $\Omega := \mathbb{R}$ and for discrete-time systems $\Omega := [-\pi/T_s, \pi/T_s)$, where T_s is the sampling time. $G(j\omega)$ will be used to denote the frequency response of the system G in both cases.

A. Integral Quadratic Constraint

Two signals p and q are said to satisfy the IQC defined by a multiplier Π , if

$$\int_{\Omega} \begin{bmatrix} \mathcal{F}_q(j\omega) \\ \mathcal{F}_p(j\omega) \end{bmatrix}^* \Pi(j\omega) \begin{bmatrix} \mathcal{F}_q(j\omega) \\ \mathcal{F}_p(j\omega) \end{bmatrix} d\omega \geq 0 \quad (1)$$

where $\mathcal{F}_p(j\omega)$ and $\mathcal{F}_q(j\omega)$ are the Fourier transform of the signals p and q respectively.

From [1, Theorem 1], the feedback connection between H , a stable LTI system with bounded infinity norm, and a bounded causal operator Δ (see Fig. 1) is stable if,

- 1) Interconnection of H and $\tau\Delta$ is well-posed, $\forall \tau \in [0, 1]$;
- 2) $\tau\Delta$ satisfies the IQC defined by Π , $\forall \tau \in [0, 1]$;
- 3) $\exists \epsilon > 0$ such that the following frequency domain inequality (FDI) is satisfied,

$$\begin{bmatrix} H(j\omega) \\ I \end{bmatrix}^* \Pi(j\omega) \begin{bmatrix} H(j\omega) \\ I \end{bmatrix} \preceq -\epsilon I, \quad \forall \omega \in \Omega \quad (2)$$

Remark 1. If Π is partitioned as

$$\Pi(j\omega) = \begin{bmatrix} \Pi_{11} & \Pi_{12} \\ \Pi_{12}^* & \Pi_{22} \end{bmatrix} (j\omega),$$

with $\Pi_{11} \succeq 0$ and $\Pi_{22} \preceq 0$, then using [1, Remark 2], $\tau\Delta$ satisfies the IQC defined by Π for all $\tau \in [0, 1]$ if and only if Δ satisfies the IQC. Most relevant IQCs can be represented in this form.

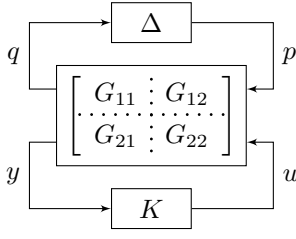


Fig. 2. Linear fractional representation of feedback system

B. Problem Description

Consider the robust control synthesis problem for the feedback connection between the perturbation Δ and the generalised plant G (see Fig. 2).

$$q = G_{11}p + G_{12}u \quad (3a)$$

$$y = G_{21}p + G_{22}u \quad (3b)$$

$$p = \Delta(q) \quad (3c)$$

$$u = Ky \quad (3d)$$

It is assumed that only the frequency response functions (FRFs) of the generalised system, which maps the perturbation $p \in \mathbb{R}^{n_p}$ and control inputs $u \in \mathbb{R}^{n_u}$ to the input of perturbation $q \in \mathbb{R}^{n_q}$ and measurements $y \in \mathbb{R}^{n_y}$,

$$G(j\omega) = \begin{bmatrix} G_{11}(j\omega) & G_{12}(j\omega) \\ G_{21}(j\omega) & G_{22}(j\omega) \end{bmatrix} \quad (4)$$

is available, where $G_{ij}(j\omega)$ are FRFs of appropriate sizes.

The frequency response of a discrete-time plant G_{22} can be estimated using the Fourier analysis method from n_u sets of finite input/output sampled data as [14]

$$G_{22}(j\omega) = \left[\sum_{k=0}^{N-1} \Upsilon(k) e^{-j\omega T_s k} \right] \left[\sum_{k=0}^{N-1} \mathbb{U}(k) e^{-j\omega T_s k} \right]^{-1} \quad (5)$$

where N is the number of data points for each experiment and T_s is the sampling period. The FRF of $G_{22}(j\omega)$ can be computed $\forall \omega \in [0, \pi/T_s]$ using (5). Each column of $\mathbb{U}(k)$ and $\Upsilon(k)$ represents, respectively, the inputs and outputs at the time sample k from one experiment, and n_u different experiments are needed to extract $G_{22}(j\omega)$ from the data. It is assumed that the input signal is persistently exciting, and the synthesis process takes into account the estimation errors caused by truncation and noise in the plant's frequency response. $G_{11}(j\omega)$, $G_{12}(j\omega)$, and $G_{21}(j\omega)$ can be determined based on the specified performance metrics, along with perturbations to be rejected according to user-defined filters and the previously computed plant $G_{22}(j\omega)$.

The objective is to synthesise a fixed-structure feedback controller $K \in \mathcal{K}$, which guarantees robustness against perturbation Δ . It is assumed that Δ satisfies the IQC defined by a known Π that meets the criteria outlined in Remark 1. Consequently, the problem can be reformulated as a feasibility problem for some $\epsilon > 0$,

$$\begin{aligned} & \text{Find } K \in \mathcal{K} & (6) \\ \text{s.t. } & \begin{bmatrix} T_{qp} \\ I \end{bmatrix}^* \Pi \begin{bmatrix} T_{qp} \\ I \end{bmatrix} (j\omega) \preceq -\epsilon I \quad \forall \omega \in \Omega & (6a) \end{aligned}$$

where,

$$T_{qp} = G_{11} + G_{12}K(I - G_{22}K)^{-1}G_{21} \quad (7)$$

III. DEVELOPMENTS

The following assumptions will be made for the generalised plant model:

(A1) $G_{21}(j\omega)$ has full row rank, $\forall \omega \in \Omega$.

(A2) $G(j\omega)$ is bounded, $\forall \omega \in \Omega$.

Remark: (A1) is related to control performance specifications, and there are similar equivalent assumptions on the rank of some matrices in model-based state space approaches [29]. It is specified to ensure that any possible disturbances have an effect on the measurements. Such a situation, from a control design perspective, indicates that either more sensors or better placement of the sensors is required for the desired objective.

In this paper, the right factorisation of the controller $K = XY^{-1}$ is considered, where $X \in \mathcal{X} \subset \mathcal{RH}_\infty$ and $Y \in \mathcal{Y} \subset \mathcal{RH}_\infty$. \mathcal{X} and \mathcal{Y} are the linear parametrisations in the optimisation variables which are chosen such that XY^{-1} reflects the choice of the desired structure of \mathcal{K} . Some examples of controller structures can be found in [26].

A. Robust Stability

The flow for the subsection aimed at achieving robust stability is as follows: Theorem 1 establishes a set of all controllers satisfying the constraint in (6a). Subsequently, Lemma 1 introduces a convex set of stabilising controllers for the nominal plant. Finally, Theorem 2 leverages the linearisation of Theorem 1 to define a convex set of robustly stabilising controllers. A special case of factorisation of Π is considered in Corollary 1 to reduce the number of LMIs for the convex set representation.

First, it is necessary to state a proposition concerning the inequality between matrices, and the pre- and post-multiplication of matrices.

Proposition 1. *Let $A = A^* \in \mathbb{C}^{n \times n}$, $B = B^* \in \mathbb{C}^{n \times n}$, and $S \in \mathbb{C}^{n \times m}$, then the following statements hold [30, Proposition 8.1.2]:*

- If $A \preceq B$, then $S^*AS \preceq S^*BS$.
- If $S^*AS \preceq S^*BS$ and S is full row rank, then $A \preceq B$.

Theorem 1. *Assume that Δ satisfies the IQC defined by Π . Furthermore, assume that only the frequency responses of the multiplier Π and the generalised model depicted in Fig. 2 are known. In that case, all controllers of the form $K = XY^{-1}$ satisfying the frequency domain inequality (6a) are also the part of the set defined by the following quadratic matrix inequality (QMI):*

$$\begin{bmatrix} (\Pi^+)^{-1} & L \\ L^* & -L^*\Pi - L \end{bmatrix} (j\omega) \succeq 0, \quad \forall \omega \in \Omega \quad (8)$$

where,

$$L = \begin{bmatrix} G_{11}\Phi + G_{12}X & G_{11}\Psi \\ \Phi & \Psi \end{bmatrix}$$

$$\Phi = G_{21}^R(Y - G_{22}X)$$

$$\Psi = I - \Phi\Phi^L = I - G_{21}^R G_{21}$$

and $\Pi^+ \succ 0$ and $\Pi^- \preceq 0$ are chosen such that

$$\Pi + \begin{bmatrix} 0 & 0 \\ 0 & \epsilon I \end{bmatrix} = \Pi^+ + \Pi^-.$$

with $\epsilon > 0$. Note that L and Φ are linear in the optimisation variables, and Ψ is known.

Proof. The nominal closed-loop transfer function T_{qp} in (7) can be written as,

$$\begin{aligned} T_{qp} &= G_{11} + G_{12}X\Phi^L = G_{11}(\Phi\Phi^L + \Psi) + G_{12}X\Phi^L \\ &= (G_{11}\Phi + G_{12}X)\Phi^L + G_{11}\Psi. \end{aligned} \quad (9)$$

Notice that Ψ is a hermitian idempotent (projector) matrix and

$$\begin{aligned} \Psi\Phi &= \Phi - \Phi\Phi^L\Phi = 0, \\ \Phi^L\Psi &= \Phi^L - \Phi^L\Phi\Phi^L = 0. \end{aligned}$$

Multiplication of $\begin{bmatrix} T_{qp} \\ I \end{bmatrix}$ by $\begin{bmatrix} \Phi & \Psi \end{bmatrix}$ results in

$$L = \begin{bmatrix} T_{qp} \\ I \end{bmatrix} \begin{bmatrix} \Phi & \Psi \end{bmatrix} = \begin{bmatrix} G_{11}\Phi + G_{12}X & G_{11}\Psi \\ \Phi & \Psi \end{bmatrix}.$$

So, the pre- and post-multiplying (6a) by $\begin{bmatrix} \Phi & \Psi \end{bmatrix}$ gives:

$$L^*\Pi L \preceq -\epsilon \begin{bmatrix} \Phi & \Psi \end{bmatrix}^* \begin{bmatrix} \Phi & \Psi \end{bmatrix} = -L^* \begin{bmatrix} 0 & 0 \\ 0 & \epsilon I \end{bmatrix} L. \quad (10)$$

Furthermore $\begin{bmatrix} \Phi & \Psi \end{bmatrix}$ can be shown to be a full row rank matrix, using

$$\mathcal{R}(\Psi) \cap \mathcal{R}(\Phi) = \{0\} \quad \text{and} \quad \text{rank}(\Psi) = n_p - \text{rank}(\Phi),$$

along with [30, Fact 2.11.9], to get

$$\text{rank} \left(\begin{bmatrix} \Phi & \Psi \end{bmatrix} \right) = \text{rank}(\Phi) + \text{rank}(\Psi) = n_p.$$

Therefore, using Proposition 1, it is possible to assert that

$$\begin{bmatrix} T_{qp} \\ I \end{bmatrix}^* \Pi \begin{bmatrix} T_{qp} \\ I \end{bmatrix} \preceq -\epsilon I \iff L^*\Pi L \preceq -L^* \begin{bmatrix} 0 & 0 \\ 0 & \epsilon I \end{bmatrix} L. \quad (11)$$

Using the fact that any square matrix can be factorised as

$$\Pi + \begin{bmatrix} 0 & 0 \\ 0 & \epsilon I \end{bmatrix} = \Pi^+ + \Pi^-$$

with $\Pi^+ \succ 0$, and $\Pi^- \preceq 0$, a sufficient condition for (6a) is:

$$L^*\Pi^+L - (-L^*\Pi^-L) \preceq 0. \quad (12)$$

Then Schur complement lemma on (12) gives the desired constraint in (8). \square

Remark 2. Observe that (11) represents a necessary and sufficient condition, indicating that the sets of controllers in the form of $K = XY^{-1}$, which satisfies (8) and (6a) respectively, are identical.

Remark 3. Note that $\Pi^- = 0$ is unattainable as it would imply that $\Pi = \Pi^+ \succ 0$, thereby rendering the satisfaction of the FDI (6a) impossible.

However, there is no guarantee that a controller in the set defined by (8) stabilises the closed-loop system. To achieve

robust stabilisation, it is essential that the controller not only satisfies the FDI in (2) but also stabilises the nominal case ($\Delta = 0$). In other words, the nominal closed-loop transfer function T_{qp} must be stable. Since it is assumed that no parametric (e.g. state-space, transfer function, etc) model is available, the closed-loop poles cannot be computed to assess the stability of the nominal closed loop. So, a sufficient condition for the stability would be derived using the Nyquist stability criterion [31].

For this purpose, the winding number $\text{wno}\{f\}$ for a real rational polynomial function $f: \mathbb{C} \mapsto \mathbb{C}$ is defined as the number of counterclockwise encirclement of $f(\delta) \in \mathbb{C}$ around the origin when $\delta \in \mathbb{C}$ traverses a contour. Two important properties of the winding number are

$$\begin{aligned} \text{wno}\{f^*\} &= \text{wno}\{f^{-1}\} = -\text{wno}\{f\} \\ \text{wno}\{fg\} &= \text{wno}\{f\} + \text{wno}\{g\} \end{aligned}$$

where $g: \mathbb{C} \mapsto \mathbb{C}$ is another real rational polynomial function, with no poles and zeros on the contour. Through Cauchy's argument principle, $\text{wno}\{f\}$ can be related to the number of poles and zeros of f inside the contour. This is used for the stability analysis of the closed-loop systems using the Nyquist stability criterion by defining an adequate Nyquist contour. The Nyquist contour for continuous-time systems is defined as the union of the imaginary axis and a semicircle with an infinite radius enclosing the right-half plane. In contrast, for discrete-time systems, the Nyquist contour is defined as the counterclockwise-oriented unit circle.

Lemma 1. Given any matrix $M \succ 0$ and the frequency response $G(j\omega)$ of a generalised model and a stabilising controller $K_c = X_c Y_c^{-1}$, a convex set of stabilising controller $K = XY^{-1}$ can be defined by the following linear matrix inequality (LMI):

$$\Phi^* M \Phi_c + \Phi_c^* M \Phi - \Phi_c^* M \Phi_c \succeq 0, \quad \forall \omega \in \Omega \quad (13)$$

where, $\Phi_c = G_{21}^R (Y_c - G_{22} X_c)$, and $\det(Y)$ and $\det(Y_c)$ have no zeros on the stability boundary.

Proof. The flow of the proof is similar to [26, Theorem 1]. First, from (13), it is noted that $\Phi^* M \Phi_c$ is a non-Hermitian strictly positive definite matrix and all its eigenvalues have strictly positive real parts. This implies that $\mathcal{W}\{\Phi^* M \Phi_c\} = 0$, where for conciseness $\mathcal{W}\{\cdot\}$ is defined as $\mathcal{W}\{\cdot\} := \text{wno}\{\det(\cdot)\}$. Note that $\mathcal{W}\{\Phi^* M \Phi_c\}$ can be expressed as:

$$\begin{aligned} \underbrace{\mathcal{W}\{\Phi^* M \Phi_c\}}_{=0} &= -\mathcal{W}\{Y - G_{22}X\} + \mathcal{W}\{Y_c - G_{22}X_c\} \\ &\quad + \mathcal{W}\{G_{21}^{R*} M G_{21}^R\} \\ &= -\mathcal{W}\{I - G_{22}K\} - \mathcal{W}\{Y\} \\ &\quad + \mathcal{W}\{I - G_{22}K_c\} + \mathcal{W}\{Y_c\} \\ &\quad + \mathcal{W}\{G_{21}^{R*} M G_{21}^R\} \end{aligned} \quad (14)$$

Since $M \succ 0$ and G_{21}^R has full column rank, $G_{21}^{R*} M G_{21}^R$ is also a strictly positive definite matrix at all frequency points [30, Proposition 8.1.2]. Therefore,

$$\mathcal{W}\{G_{21}^{R*} M G_{21}^R\} = 0 \quad (15)$$

Given that K_c is assumed to be a stabilising controller and using the Nyquist theorem, $\mathcal{W}\{I - G_{22}K_c\} = N_{G_{22}} + N_{K_c}$,

where $N_{G_{22}}$ is the number of unstable poles of G_{22} , and N_{K_c} is the number of unstable poles of K_c . Furthermore, since $Y, Y_c \in \mathcal{RH}_\infty$, $\mathcal{W}\{Y\} = -N_K$ and $\mathcal{W}\{Y_c\} = -N_{K_c}$, where N_K is the number of unstable poles of the controller K . It can be seen that,

$$\mathcal{W}\{I - G_{22}K\} = N_{G_{22}} + N_{K_c}.$$

Hence, all controllers K in the set stabilises the closed-loop system. \square

Remark 4. *The relaxations concerning zeros on the stability boundary, and the avoidance of unstable zero-pole cancellation in $G_{22}K$, can be demonstrated using a similar approach as detailed in [26, Remark 1 and 2].*

Theorem 2. *In addition to the assumptions of Theorem 1, assume that $K_c = X_c Y_c^{-1}$ is a known stabilising controller for the nominal plant, then a convex set of robustly stabilising controllers against the bounded causal operator Δ is defined by the following LMIs:*

$$\begin{bmatrix} (\Pi^+)^{-1} & L \\ L^* & -\mathcal{L} \end{bmatrix} (j\omega) \succeq 0, \quad \forall \omega \in \Omega \quad (16)$$

$$(\Phi^* \Phi_c + \Phi_c^* \Phi - \Phi_c^* \Phi_c)(j\omega) \succeq 0, \quad \forall \omega \in \Omega \quad (17)$$

where,

$$\begin{aligned} \mathcal{L} &= L^* \Pi^- L_c + L_c^* \Pi^- L - L_c^* \Pi^- L_c \\ L_c &= \begin{bmatrix} G_{11} \Phi_c + G_{12} X_c & G_{11} \Psi \\ \Phi_c & \Psi \end{bmatrix} \end{aligned}$$

Proof. The proof relies on finding a convex lower bound on the result of Theorem 1 and using the result of Lemma 1 to ensure the stability of the nominal system. The convex-concave component of the constraint $L^* \Pi^- L$ can be convexified around a known controller $K_c = X_c Y_c^{-1}$ such that

$$(L - L_c)^* \Pi^- (L - L_c) \preceq 0 \quad (18)$$

$$\implies L^* \Pi^- L \preceq L^* \Pi^- L_c + L_c^* \Pi^- L - L_c^* \Pi^- L_c = \mathcal{L}. \quad (19)$$

So, the convex lower bound on the constraint is,

$$\begin{bmatrix} (\Pi^+)^{-1} & L \\ L^* & -L^* \Pi^- L \end{bmatrix} \succeq \begin{bmatrix} (\Pi^+)^{-1} & L \\ L^* & -\mathcal{L} \end{bmatrix} \succ 0$$

Selecting a stabilising controller as K_c and $M = I$, Lemma 1 gives a sufficient condition for the stability of the nominal closed-loop,

$$\Phi^* \Phi_c + \Phi_c^* \Phi - \Phi_c^* \Phi_c \succeq 0. \quad \square$$

The inherent conservatism in the theorem stems from the inner approximation detailed in (18), and this conservatism diminishes as equality is achieved. To minimise this conservatism for any given L and L_c , Π^- can be chosen to be as small as possible. Furthermore, it is worth noting that up to this point, no assumptions have been imposed on the structure of Π . However, it can be shown that by introducing a particular structure for Π , as outlined in Remark 1, it is possible to eliminate one of the LMIs with very minimal additional conservatism.

Corollary 1. *Assume that Π is partitioned as outlined in Remark 1, then a convex set of robustly stabilising controllers against the bounded causal operator Δ is defined by the following LMI:*

$$\begin{bmatrix} (\Pi^+)^{-1} & L \\ L^* & -\mathcal{L} \end{bmatrix} (j\omega) \succeq 0, \quad \forall \omega \in \Omega \quad (20)$$

with some $\alpha, \beta \geq 0$ such that $\Pi_{22} - \beta I \prec 0$ and

$$\Pi^+ = \begin{bmatrix} \Pi_{11} + \alpha I & \Pi_{12} \\ \Pi_{12}^* & (\beta + \epsilon) I \end{bmatrix} \succ 0$$

where,

$$\mathcal{L} = \begin{bmatrix} \mathcal{L}_{11} & \mathcal{L}_{12} \\ \mathcal{L}_{12}^* & \mathcal{L}_{22} \end{bmatrix}$$

$$\begin{aligned} \mathcal{L}_{11} &= \Phi^* (\Pi_{22} - \beta I) \Phi_c + \Phi_c^* (\Pi_{22} - \beta I) \Phi \\ &\quad - \Phi_c^* (\Pi_{22} - \beta I) \Phi_c \end{aligned}$$

$$\mathcal{L}_{12} = \Phi^* (\Pi_{22} - \beta I) \Psi - \alpha (G_{11} \Phi + G_{12} X)^* G_{11} \Psi$$

$$\mathcal{L}_{22} = \Psi (\Pi_{22} - \beta I) \Psi - \alpha (G_{11} \Psi)^* G_{11} \Psi$$

Proof. It can be easily verified that $\exists \alpha, \beta \geq 0$ such that

$$\Pi^+ = \begin{bmatrix} \Pi_{11} + \alpha I & \Pi_{12} \\ \Pi_{12}^* & (\beta + \epsilon) I \end{bmatrix} \succ 0 \quad \text{and} \quad \Pi_{22} - \beta I \prec 0.$$

This choice of Π^+ gives,

$$\Pi^- = \begin{bmatrix} -\alpha I & 0 \\ 0 & \Pi_{22} - \beta I \end{bmatrix} \quad \text{and} \quad L^* \Pi^- L = \begin{bmatrix} \mathcal{L}'_{11} & \mathcal{L}_{12} \\ \mathcal{L}_{12}^* & \mathcal{L}_{22} \end{bmatrix}$$

where,

$$\begin{aligned} \mathcal{L}'_{11} &= \Phi^* (\Pi_{22} - \beta I) \Phi - \alpha (G_{11} \Phi + G_{12} X)^* (G_{11} \Phi + G_{12} X) \\ &\preceq \Phi^* (\Pi_{22} - \beta I) \Phi \end{aligned} \quad (21)$$

The upper bound can be convexified around a known controller $K_c = X_c Y_c^{-1}$ with $M = \Pi_{22} - \beta I \prec 0$ such that

$$\begin{aligned} &(\Phi - \Phi_c)^* M (\Phi - \Phi_c) \preceq 0 \\ \implies &\Phi^* M \Phi \preceq \Phi^* M \Phi_c + \Phi_c^* M \Phi - \Phi_c^* M \Phi_c = \mathcal{L}_{11}. \end{aligned}$$

This upper bound can then be used to find a convex lower bound on the constraint of Theorem 1,

$$\begin{bmatrix} (\Pi^+)^{-1} & L \\ L^* & -L^* \Pi^- L \end{bmatrix} \succeq \begin{bmatrix} (\Pi^+)^{-1} & L \\ L^* & -\mathcal{L} \end{bmatrix} \succeq 0.$$

Furthermore, notice that the sufficient condition for stability from Lemma 1 is satisfied by the convex bound $\mathcal{L}_{11} \succ 0$. \square

Remark 5. *Note that additional conservatism in the relaxation (21) diminishes as α approaches 0. When $\Pi_{11} \succ 0$, choosing $\alpha = 0$ eliminates any additional conservatism.*

Conventional IQCs: The authors present a subset of conventional IQCs along with their respective Π^+ and Π^- counterparts with the expectation of bolstering the versatility of the proposed approach in addressing diverse perturbation scenarios.

a) \mathcal{H}_∞ bounded perturbation : For the perturbations which are upper bounded by some $\gamma > 0$, $\Pi(j\omega)$ can be defined as [1]:

$$\Pi = \begin{bmatrix} \gamma^2 I & 0 \\ 0 & -I \end{bmatrix}. \quad (22)$$

A feasible factorisation can be given as,

$$\Pi^+ = \begin{bmatrix} \gamma^2 I & 0 \\ 0 & \epsilon I \end{bmatrix} \quad \text{and} \quad \Pi^- = \begin{bmatrix} 0 & 0 \\ 0 & -I \end{bmatrix}$$

Then, the condition in Theorem 1 can be written as,

$$\begin{bmatrix} \gamma^{-2} I & 0 & \vdots & G_{11}\Phi + G_{12}X & G_{11}\Psi \\ 0 & \epsilon^{-1} I & \vdots & \Phi & \Psi \\ \dots & \dots & \dots & \dots & \dots \\ \star & \vdots & \vdots & \Phi^*\Phi & 0 \\ \vdots & \vdots & \vdots & 0 & \Psi \end{bmatrix} \succ 0 \quad (23)$$

using the fact that $\Phi^*\Psi = \Psi\Phi = 0$.

Corollary 2 (\mathcal{H}_∞ performance). *The IQC defined by (22) yields the closed loop transfer function T_{qp} , which has the \mathcal{H}_∞ norm upper bounded by $\gamma_p = \gamma^{-1}\sqrt{1-\epsilon}$, and (23) is equivalent to the constraint presented in Eq. (12) of [26],*

$$\begin{bmatrix} \gamma_p^2 I - (G_{11}\Psi)(G_{11}\Psi)^* & G_{11}\Phi + G_{12}X \\ (G_{11}\Phi + G_{12}X)^* & \Phi^*\Phi \end{bmatrix} \succeq 0.$$

Proof. See Appendix. \square

Remark 6. *This equivalence with the result of [26] enables us to infer that this representation of the IQC's FDI does not introduce additional conservatism into the solution, and the comprehensive comparison results outlined in [26] are equally applicable here.*

b) *Input-output passivity:* The transfer function T_{qp} is strictly input passive if

$$\Pi = \begin{bmatrix} 0 & -I \\ -I & 0 \end{bmatrix}. \quad (24)$$

For some $\beta \geq 0$, a feasible factorisation can be given as,

$$\Pi^+ = \begin{bmatrix} I & -I \\ -I & (1 + \beta + \epsilon)I \end{bmatrix} \quad \text{and} \quad \Pi^- = \begin{bmatrix} -I & 0 \\ 0 & -(1 + \beta)I \end{bmatrix}.$$

c) *Constant real scalar:* If Δ is defined as multiplication by a real scalar ≤ 1 , then Δ satisfies all IQCs defined by

$$\Pi = \begin{bmatrix} V_1(j\omega) & V_2(j\omega) \\ V_2(j\omega)^* & -V_1(j\omega) \end{bmatrix} \quad (25)$$

where $V_1(j\omega) \succ 0$ and $V_2(j\omega) = -V_2(j\omega)^*$ are bounded and measurable matrix functions.

A feasible factorisation can be given for some $\beta \geq 0$,

$$\Pi^+ = \begin{bmatrix} V_1 & V_2 \\ V_2^* & (\epsilon + \beta)I \end{bmatrix} \succ 0 \quad \text{and} \quad \Pi^- = \begin{bmatrix} 0 & 0 \\ 0 & -V_1 - \beta I \end{bmatrix}.$$

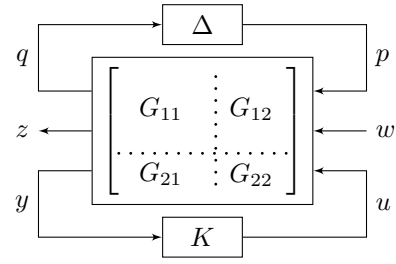


Fig. 3. Linear fractional representation of feedback system with performance channels

d) *Memoryless sector non-linearity:* Let Δ be a function such that,

$$aq^2 \leq \Delta(q)q \leq bq^2, \quad \forall q \quad (26)$$

then Δ satisfies the IQC defined by

$$\Pi = \begin{bmatrix} -2ab & a + b \\ a + b & -2 \end{bmatrix} \quad (27)$$

If $a < 0 < b$, a feasible factorisation can be given for some $\beta \geq 0$,

$$\Pi^+ = \begin{bmatrix} -2ab & a + b \\ a + b & \beta + \epsilon \end{bmatrix} \succ 0 \quad \text{and} \quad \Pi^- = \begin{bmatrix} 0 & 0 \\ 0 & -2 - \beta \end{bmatrix}.$$

B. Robust Performance

To consider the robust performance, an additional performance channel is added as depicted in Fig. 3. The new feedback is now defined through the following linear fractional representation,

$$\begin{bmatrix} q \\ z \\ y \end{bmatrix} = \begin{bmatrix} G_{11} & \vdots & G_{12} \\ \dots & \dots & \dots \\ G_{21} & \vdots & G_{22} \end{bmatrix} \begin{bmatrix} p \\ w \\ u \end{bmatrix} \quad (28a)$$

$$p = \Delta(q) \quad (28b)$$

$$u = Ky \quad (28c)$$

As shown in Corollary 2, performance metrics can be represented using an equivalent IQC multipliers. Let the performance metric under consideration satisfy the IQC defined by $\Pi_p(\gamma)$ where γ_p represents the performance index. Then a composite IQC can be defined for the robust performance as

$$\Pi_{rp}(\gamma_p) = \begin{bmatrix} \Pi_{11} & 0 & \vdots & \Pi_{12} & 0 \\ 0 & \Pi_{p,11}(\gamma_p) & \vdots & 0 & \Pi_{p,12}(\gamma_p) \\ \dots & \dots & \dots & \dots & \dots \\ \Pi_{12}^* & 0 & \vdots & \Pi_{22} & 0 \\ 0 & \Pi_{p,12}^*(\gamma_p) & \vdots & 0 & \Pi_{p,22}(\gamma_p) \end{bmatrix}. \quad (29)$$

Corollary 3 (Robust Performance). *The interconnection (28) is robustly stable to Δ and has robust performance with respect to $\Pi_p(\gamma_p)$ on the channel $w \rightarrow z$, if there exist $K \in \mathcal{K}$ such that*

$$\begin{bmatrix} T \\ I \end{bmatrix}^* \Pi_{rp}(\gamma_p) \begin{bmatrix} T \\ I \end{bmatrix} (j\omega) \prec 0, \quad \forall \omega \in \Omega \quad (30)$$

where,

$$T = G_{11} + G_{12}K(I - G_{22}K)^{-1}G_{21}$$

Proof. Let T be partitioned as,

$$T = \begin{bmatrix} T_{qp} & T_{qw} \\ T_{zp} & T_{zw} \end{bmatrix}. \quad (31)$$

Then using simple row and column permutations, it can be shown that the condition can be rewritten as

$$\begin{bmatrix} T_{qp} & T_{qw} \\ I & 0 \\ \dots & \dots \\ T_{zp} & T_{zw} \\ 0 & I \end{bmatrix}^* \begin{bmatrix} \Pi & 0 \\ 0 & \Pi_p(\gamma_p) \end{bmatrix} \begin{bmatrix} T_{qp} & T_{qw} \\ I & 0 \\ \dots & \dots \\ T_{zp} & T_{zw} \\ 0 & I \end{bmatrix} \prec 0. \quad (32)$$

From [9, Corollary 3], it can be shown that the closed loop has the robust performance γ_p against the perturbation Δ which satisfies the IQC defined by Π . \square

Analogous to the previous section, the controller synthesis problem for robust performance can be reformulated as a convex optimisation problem over some performance index γ_p using IQC formulation.

$$\begin{aligned} & \min_{K \in \mathcal{K}} \gamma_p & (33) \\ \text{s.t.} & \begin{bmatrix} T \\ I \end{bmatrix}^* \Pi_{rp}(\gamma_p) \begin{bmatrix} T \\ I \end{bmatrix} (j\omega) \prec 0 \quad \forall \omega \in \Omega \end{aligned}$$

C. Implementation Remarks

Frequency sampling: The problems presented in the paper are formulated as frequency domain inequalities in a convex semi-infinite program (SIP). One of the common approach to solve SIPs is to sample the infinite number of constraints in Ω at a reasonably large finite set of frequencies $\Omega_N = \{\omega_1, \dots, \omega_N\} \subset \Omega$. Since all constraints are applied on the Hermitian matrices, constraints will also be satisfied for all negative frequencies. The formulated optimisation problems are convex, and large values of N can be handled by numerical solvers. This sampling approach implies that constraint satisfaction for all frequency points is no longer guaranteed, and could potentially result in non-robust controllers. Nonetheless, since the optimisation is convex, the scenario approach can be employed to provide a probabilistic guarantee of the robustness [32]. In practice, choosing a sufficiently large number of frequency points results in a robust controller.

Iterative procedure: An initial stabilising controller is required for the convexification process in Theorem 2. It is possible that the convexified set of the stabilising controller for the nominal case and the convexified set of the IQC constraint do not intersect. To address this issue, a slack variable can be introduced to the IQC constraint and optimised over.

$$\begin{aligned} & \min_{K \in \mathcal{K}} \nu & (34) \\ \text{s.t.} & \begin{bmatrix} (\Pi^+)^{-1} & L \\ L^* & -\mathcal{L} \end{bmatrix} (j\omega) \succeq -\nu I \quad \forall \omega \in \Omega \\ & (\Phi^* \Phi_c + \Phi_c^* \Phi - \Phi_c^* \Phi_c)(j\omega) \succeq 0 \quad \forall \omega \in \Omega \end{aligned}$$

Subsequently, the problem can be addressed in an iterative fashion, employing the optimal controller from each iteration

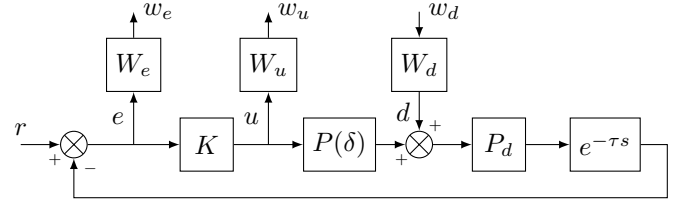


Fig. 4. Block diagram of the mixed sensitivity problem

as the initial controller for the subsequent one. The slack is non-increasing as the initial controller is always a feasible solution and the problem is convex. So, this series of optimisations would converge to a robust controller, if it exists.

Robustness with performance: For synthesis of a robust controller with a specified performance metric, it is recommended to initially optimise for the optimal nominal performance. Following that, optimise to identify a robust controller employing the slacked IQC constraint, and finally optimise again to achieve the best nominal performance while ensuring robustness with the strict IQC constraint.

D. Simulation Results

The control synthesis approach is applied to a mixed sensitivity problem proposed in [33], which is shown in Fig. 4. The uncertain plant and the disturbance model are defined as:

$$P(\delta) = \frac{4}{s^2 + 0.1(1 + 0.5\delta)s + (1 + 0.5\delta)^2}, \quad P_d = \frac{10}{s + 0.1}.$$

Additionally, a measurement delay of 0.025 s at most is also considered. The synthesis objective are chosen with the aim of tracking the reference signal r and rejecting the disturbance signal d at low frequencies by employing the performance filters as $W_e = \frac{2(s+3.674)^2}{3(s+0.03)^2}$, $W_u = \frac{s+10}{s+10^4}$, and $W_d = 1$.

The uncertainty in the plant is extracted to a multiplication by a constant real scalar which satisfies the IQC defined by Π in (25). The uncertainty in measurement delay is represented as the uncertainty in the time-difference operator which satisfies the IQC defined by [34]

$$\Pi = \begin{bmatrix} \begin{bmatrix} \phi(j\omega)V_{11} \\ \psi(j\omega)V_{12} \\ s\tau_0 V_{13} \end{bmatrix}^* \begin{bmatrix} \phi(j\omega)V_{11} \\ \psi(j\omega)V_{12} \\ s\tau_0 V_{13} \end{bmatrix} & 0 \\ 0 & -\sum_{i=1}^3 V_i^* V_i \end{bmatrix}$$

where, τ_0 is the maximum delay, and $\exists c, d > 0$

$$\begin{aligned} \phi(j\omega) &= 2 \frac{\tau_0^2 s^2 + c\tau_0 s}{\tau_0^2 s^2 + 2\sqrt{c}\tau_0 s + 2c} \\ \psi(j\omega) &= 2 \frac{\tau_0^2 s^2 + \sqrt{12.5}\tau_0 s}{\tau_0^2 s^2 + \sqrt{6.5 + 2\sqrt{50}}\tau_0 s + \sqrt{50}} + d \end{aligned}$$

The controller is computed with $V_1(j\omega) = I$ and $V_2(j\omega) = 0$ for robustness to plant uncertainty, and $V_{11} = 0.7$, $V_{12} = 1$, $V_{13} = 7$, $c = 2$, and $d = 10^{-6}$ for robustness to measurement delay. The nominal performant robust controller

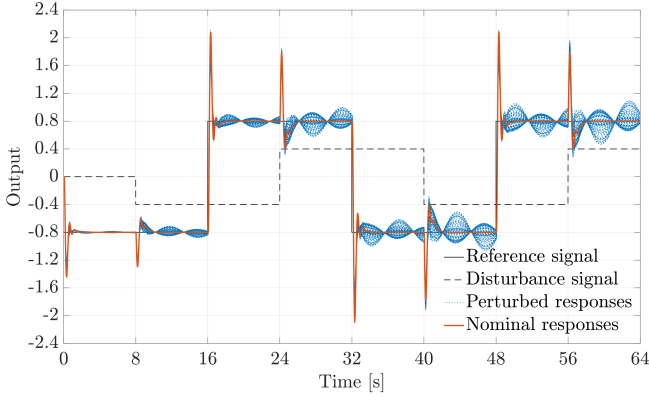


Fig. 5. Time-domain simulation results for random samples

obtained from the proposed synthesis approach by optimising over 450 points between 10^{-4} Hz and 10^4 Hz is

$$K = \begin{bmatrix} -0.009 & 0.059 & -0.002 & 0.482 & -0.137 & -3.895 \\ -0.059 & -0.362 & 0.015 & -53.633 & 2.448 & -10.553 \\ 0.002 & 0.015 & -0.001 & 18.042 & -0.113 & 0.411 \\ 0.482 & 53.633 & -18.042 & -56.590 & 24.666 & 121.294 \\ -0.137 & -2.448 & 0.113 & 24.666 & -22.258 & -30.755 \\ -3.895 & 10.553 & -0.411 & 121.294 & -30.755 & 1.768 \end{bmatrix}.$$

In Fig. 5, the time-domain simulation results for the synthesised controller are shown for 100 samples of the uncertainty. The root mean square values of the nominal and worst-case simulated tracking errors are 0.2002 and 0.2354 respectively.

IV. NON-PARAMETRIC IQC MULTIPLIERS

Until now, the focus has primarily revolved around the IQC defined through parametric multipliers. Nevertheless, the developments presented in this paper extend to include non-parametric IQC multipliers. This section provides an illustrative example regarding the identification of a non-parametric IQC multiplier using experimental frequency-domain data. To validate these developments, a previously published result [35] is implemented with the method outlined in Section III-A. The subsequent section offers a concise summary of the content presented in [35].

The primary objective of using non-parametric IQC multipliers is to reduce conservatism in uncertainty modelling and to compute a robust controller with high nominal performance. The uncertain plant under consideration is represented using a non-parametric nominal model coupled with an additive uncertainty set. Classically, the nominal model is selected by choosing one measurement from multiple identification experiments, or alternatively, by averaging over all the experiments. The uncertainty set is then determined by computing the smallest disk encompassing all realisations. In this work, given a set of frequency responses for a multiple-input multiple-output (MIMO) LTI system, a ‘best’ nominal model and the associated additive elliptical uncertainty set, which is consistent with the data, is identified. The controller synthesis objective is to design a robust controller with high nominal performance for the system in Fig. 6. Utilising a split representation, a corresponding non-parametric IQC multiplier is constructed

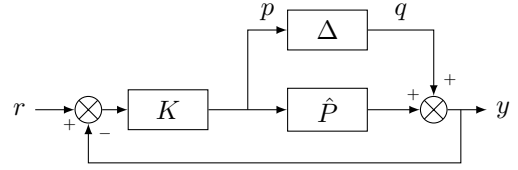


Fig. 6. Feedback system with additive uncertainty block

which can be employed using the methodology proposed in this paper.

A. Optimal Additive Uncertainty Set

An optimal non-parametric additive uncertainty set represented as elementwise elliptical uncertainty is computed using tools from convex optimisation. The systems under consideration are linear time-invariant (LTI) plants represented using FRF $\{P^i(j\omega)\}$ which can be obtained from a series of m experiments using the Fourier analysis on the sampled input-output data as presented in [14].

Definition 1. A frequency response function (FRF) matrix with the elementwise additive elliptical uncertainty set can be represented as $\mathcal{M}(\hat{P}, A)(j\omega) \triangleq \hat{P}(j\omega) + \Delta$, where $\hat{P}(j\omega)$ is the nominal FRF model and Δ is the additive uncertainty set characterised by a matrix A . The element Δ_{kl} of Δ represents the additive uncertainty of $\hat{P}_{kl}(j\omega)$ from the input channel l to the output channel k and belongs to the following elliptical set:

$$\|A_{kl}(\omega)\mathcal{C}(\Delta_{kl})\|_2 \leq 1, \quad \forall k, l \quad (35)$$

where $A_{kl}(\omega) \in \mathbb{R}^{2 \times 2}$ represents the ellipse parameters and $\mathcal{C}(\Delta_{kl}) \in \mathbb{R}^{2 \times 1}$ is defined in Notions. The total area of the uncertainty of $\mathcal{M}(\hat{P}, A)(j\omega)$ is given as $\sum_k \sum_l \pi \det\{A_{kl}^{-1}(\omega)\}$.

The uncertainty set can be obtained by a convex optimisation problem with a log-det objective and a conic constraint for each measurement in the dataset at all frequencies and for each input-output pair. In practical implementation, since the optimisation for controller synthesis will be performed at a finite set of frequency points Ω_N the following optimisation needs to be solved at these finite number of points:

$$\begin{aligned} \min_{A_{kl}, b_{kl}} & -\log \det\{A_{kl}(\omega_n)\} \\ \text{s.t.} & \|A_{kl}(\omega_n)\mathcal{C}(P_{kl}^i(j\omega_n)) - b_{kl}(\omega_n)\|_2 \leq 1 \quad \forall i \end{aligned} \quad (36)$$

Note that, in general, the best FRF might not be any of the measured FRF of the system or their average.

Remark 7. For the matrix $A_{kl}^\circ(\omega)$ to be finite, the area of the elliptical uncertainty should be non-zero. So, there should exist at least three non-colinear points. The presence of noise, in practical scenarios, makes it improbable for this assumption to be violated.

B. IQC multiplier

In this section, the uncertainty set of $\mathcal{M}(\hat{P}, A^\circ)$ is shown to satisfy the IQC defined by a non-parametric multiplier Π .

Consider a transformation matrix

$$J = \begin{bmatrix} 1 & 0 \\ 0 & j \end{bmatrix} \quad \text{with} \quad J^* J = I.$$

From the definition of $\mathcal{M}(\hat{P}, A^\circ)$, Δ_{kl} satisfies

$$\begin{aligned} \|A_{kl}^\circ(\omega) \mathcal{C}(\Delta_{kl})\|_2 &\leq 1 \quad \forall \omega \\ \Leftrightarrow \|A_{kl}^\circ(\omega) J^* \mathcal{C}(\Delta_{kl})\|_2 &\leq 1 \quad \forall \omega \end{aligned}$$

where, $\mathcal{C}(\Delta_{kl}) = J \mathcal{C}(\Delta_{kl})$. This can be written as,

$$\begin{bmatrix} 1 \\ \mathcal{C}(\Delta_{kl}) \end{bmatrix}^* \begin{bmatrix} 1 & 0 \\ 0 & -\bar{A}_{kl}^*(j\omega) \bar{A}_{kl}(j\omega) \end{bmatrix} \begin{bmatrix} 1 \\ \mathcal{C}(\Delta_{kl}) \end{bmatrix} \geq 0, \quad \forall \omega$$

where $\bar{A}_{kl}(j\omega) = A_{kl}^\circ(\omega) J^*$. So, the uncertainty can be shown to satisfy the IQC defined by

$$\Pi_{kl}(j\omega) = \begin{bmatrix} 1 & 0 \\ 0 & -\bar{A}_{kl}^*(j\omega) \bar{A}_{kl}(j\omega) \end{bmatrix}. \quad (37)$$

Note that $\Pi_{kl}(j\omega)$ is a dynamic multiplier for the elliptical uncertainty set, in contrast to the frequency-dependent static gain for the disk uncertainty set. Since the multiplier satisfies the condition of Remark 1, $\tau \mathcal{C}(\Delta_{kl})$ also satisfies the IQC defined by Π_{kl} for all $\tau \in [0, 1]$. For robust controller synthesis, a single IQC for the full uncertainty block Δ is needed. By abuse of notation, denote

$$\mathcal{C}(\Delta) = \begin{bmatrix} \text{Re}\{\Delta\} \\ j \text{Im}\{\Delta\} \end{bmatrix}.$$

It is well-known that operators with diagonal structure, in which each sub-operator meets the IQC defined by a certain multiplier, also meet the IQC defined by a structured multiplier [13]. Up till now, the multipliers have been generated for each input-output channel, and the aim is to find a transformation from the MIMO uncertainty block to a diagonally structured uncertainty. So, the representation $\mathcal{C}(\Delta) = W_L \mathcal{D} W_R$ where, $\mathcal{D} = \text{diag}(\mathcal{C}(\Delta_{11}), \mathcal{C}(\Delta_{12}), \dots, \mathcal{C}(\Delta_{n_y n_u}))$ is desired. It can be verified that

$$W_L = \begin{bmatrix} I_{n_y} \otimes 1_{1 \times n_u} \otimes \begin{bmatrix} 1 & 0 \\ 0 & 1 \end{bmatrix} \\ I_{n_y} \otimes 1_{1 \times n_u} \otimes \begin{bmatrix} 1 & 0 \\ 0 & 1 \end{bmatrix} \end{bmatrix} \quad \text{and} \quad W_R = 1_{n_y \times 1} \otimes I_{n_u}$$

satisfies this desired representation. Then, it can be shown that \mathcal{D} satisfies the IQC defined by

$$\Pi(j\omega) = \begin{bmatrix} I & 0 \\ 0 & -\bar{A}^* \bar{A} \end{bmatrix} (j\omega)$$

where, $\bar{A} = \text{diag}(\bar{A}_{11}, \bar{A}_{12}, \dots, \bar{A}_{n_y n_u})$. A feasible factorisation of $\Pi(j\omega)$ can be given as,

$$\Pi^+ = \begin{bmatrix} I & 0 \\ 0 & \epsilon I \end{bmatrix} \quad \text{and} \quad \Pi^- = \begin{bmatrix} 0 & 0 \\ 0 & -\bar{A}^* \bar{A} \end{bmatrix}.$$

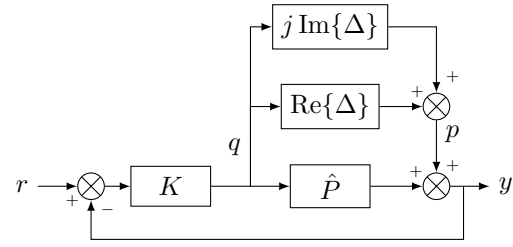


Fig. 7. Feedback system with split additive uncertainty block

C. Robust synthesis

A robust controller K is to be synthesised which stabilizes the closed-loop system against the uncertainty Δ described by $\mathcal{M}(\hat{P}, A^\circ)$, as depicted in Fig. 6. For the uncertainty models described by $\mathcal{M}(\hat{P}, A^\circ)$, the uncertainty block can be split and structured as shown in Fig. 7.

Using the representation $\mathcal{C}(\Delta) = W_L \mathcal{D} W_R$, an equivalent LFR formulation for robust controller synthesis against the uncertainty \mathcal{D} can be given as,

$$\begin{bmatrix} q \\ y \end{bmatrix} = \begin{bmatrix} \dots & 0 & \dots & W_R \\ \dots & -[I \ I] W_L & \dots & -\hat{P} \end{bmatrix} \begin{bmatrix} \tilde{p} \\ u \end{bmatrix} \quad (38a)$$

$$\tilde{p} = \mathcal{D} q \quad (38b)$$

$$u = K y \quad (38c)$$

where \tilde{p} is the virtual output of the structured uncertainty \mathcal{D} . Incorporating the IQC constraint in Theorem 2 for the multiplier into the performance problem described in [26] results in the synthesis of a robust controller with nominal performance.

V. EXPERIMENTAL RESULTS

In this section, a robust controller is synthesized for a hybrid active-passive micro-vibration damping platform (MIVIDA). The aim is to mitigate micro-disturbances and isolate the sensitive optical payload from external disturbances. The primary goal of the MIVIDA platform is stabilisation of vibration-sensitive payloads against multiple unknown external perturbations inherent in the satellites. The modular platform comprises of an adjustable number of passive dampers, a set of proof mass actuators (PMA) creating a 6 degree of freedom (DoF) force tensor, and a payload interface capable of accommodating various types of sensitive instruments. To actively counteract disturbances transmitted from the satellite body, the platform utilises the accelerometer measurements in close proximity to the payload. An image of the system is presented in Fig. 8. All experimental tests with the platform are conducted at the Microvibration Characterisation Facility at CSEM in Neuchâtel, Switzerland [36].

Due to the modular design, the FRF of the passive system stage can significantly vary depending on the applied screw torque and other mechanical system properties. A controller is designed for a configuration where the actuators are placed along the main axes having two parallel actuators per axis. In addition, three accelerometers (one along each axis) are mounted for local measurement of the disturbances at the

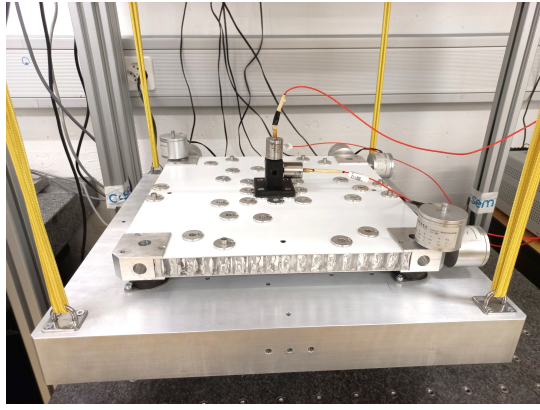


Fig. 8. Hybrid micro-disturbance isolation platform developed at CSEM, Switzerland

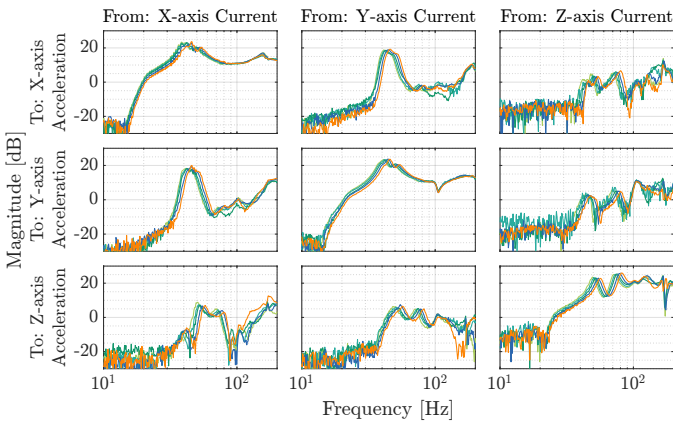


Fig. 9. Multi-model FRF from uncertain screw torque

payload interface. The parallel nature of the actuator placement together with the three accelerometers leads to a MIMO system with three inputs and three outputs. A multimodel FRF is acquired from five different experiments with different screw torques in the interval from 6 N m to 8 N m. The resulting FRFs are presented in Fig. 9. The screw torque directly influences the rigidity of the system, which can be seen by the shift in the frequency of the first mode in the interval 45 Hz to 60 Hz.

The aim is to design a robust controller using the proposed approach, focusing on effectively rejecting a sinusoidal perturbation at a frequency of 80 Hz. The generalised system for robustness and performance can be respectively specified as:

$$G_r = \begin{bmatrix} \dots & 0 & \dots & W_R \\ \dots & \dots & \dots & \dots \\ -[I & I] & W_L & \dots & -\hat{P} \end{bmatrix}, \quad G_p = \begin{bmatrix} W & -W\hat{P} \\ \dots & \dots \\ I & -\hat{P} \end{bmatrix}$$

where, \hat{P} is the identified nominal plant, W_R and W_L are matrices as defined in section IV. The performance weighting filter W is chosen as a peak filter with a centre frequency of

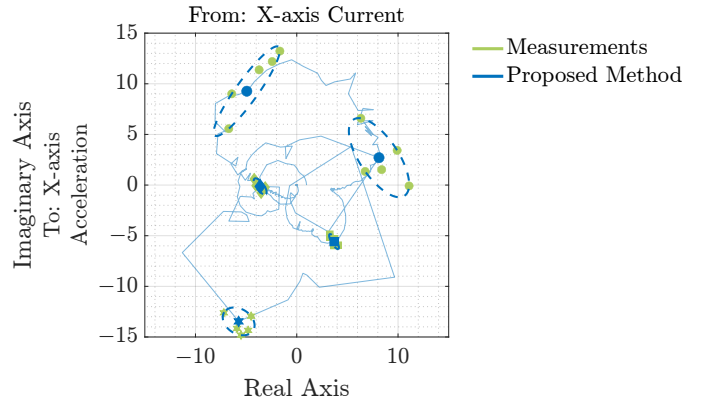


Fig. 10. Nyquist plot of the estimated model using the proposed method. Dashed lines shows the estimated uncertainty boundary.

TABLE I
RESULTING ATTENUATION PERFORMANCE ALONG THE DIFFERENT AXES

	X-axis	Y-axis	Z-axis
Attenuation Performance [dB]	13.61	6.63	9.80

80 Hz. The complete optimisation problem to be solved is,

$$\begin{aligned} & \min_{X, Y, \gamma} \gamma & (39) \\ \text{s.t.} & \begin{bmatrix} \gamma I - \Lambda_p & G_{p,11}\Phi_p^* + G_{p,12}X \\ \star & \Phi_p^*\Phi_{p,c} + \Phi_{p,c}^*\Phi_p - \Phi_{p,c}^*\Phi_{p,c} \end{bmatrix} (j\omega) \succ 0, \\ & \begin{bmatrix} (\Pi^+)^{-1} & L \\ L^* & -\mathcal{L} \end{bmatrix} (j\omega) \succeq 0, \\ & \forall \omega \in \Omega \end{aligned}$$

with Π^+ and Π^- chosen as specified in Section IV.

The controller successfully attains the desired robust performance, with an infinity norm of 0.5079. It is important to mention that the controller synthesised in this study differs from the one presented in [35]. Nevertheless, they deliver similar performance, given the inherent non-uniqueness of \mathcal{H}_∞ controllers.

The designed controller was implemented and tested on the platform for a sinusoidal perturbation at a frequency of 80 Hz injected using an external shaker along the x-axis. The achieved performance of the controller is presented in Fig. 11. An attenuation of 13.18 dB along the perturbation axis can be achieved. The resulting attenuation performances are summarised in Table I.

The traditional method, which employs the disk-based uncertainty quantification, results in a less performant controller, largely due to the larger uncertainty bounds leading to increased conservatism [35]. It is important to recognise the fact that the use of the elliptical uncertainty bound quantification is only feasible because of the non-parametric nature of the IQC multiplier.

VI. CONCLUSION

A novel controller synthesis approach has been devised for designing robust controllers, using only frequency-domain

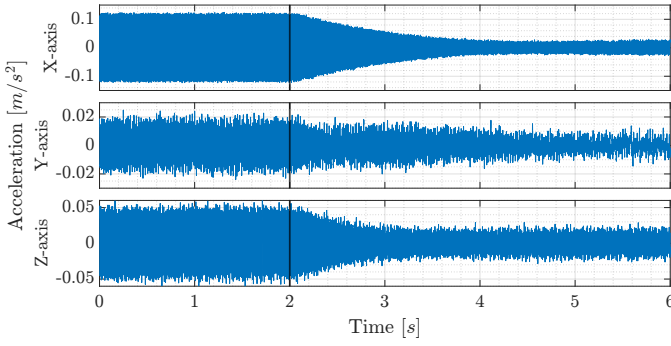


Fig. 11. Attenuation performance for the synthesised controller by comparison of open-loop (from 0s to 2s) with the closed-loop system (after 2s)

data of a generalised MIMO system. The resulting controller ensures robust stability or robust performance guarantees for perturbations described by IQC. The control synthesis is facilitated through iterative convex optimisations with LMI constraints. Furthermore, it has been demonstrated that the proposed approach can be applied even with non-parametric IQC multipliers.

The method is first verified in simulation using an uncertain LTI plant with uncertain bounded measurement delay. The resulting robust controller has a similar performance compared to the controller obtained in [33]. A high-performance controller, designed to be robust to non-parametric uncertainty quantification, is applied to the hybrid micro-vibration damping platform MIVIDA for validation. The attained performance closely aligns with the results presented in [35].

APPENDIX

Proof of Corollary 2: \mathcal{H}_∞ performance

Proof. By expressing the constraint in (6a) using (22), the desired specification is straightforwardly obtained.

$$\begin{aligned} \begin{bmatrix} T_{qp} \\ I \end{bmatrix}^* \begin{bmatrix} \gamma^2 I & 0 \\ 0 & -I \end{bmatrix} \begin{bmatrix} T_{qp} \\ I \end{bmatrix} (j\omega) &\preceq -\epsilon I & \forall \omega \in \Omega \\ T_{qp}^*(j\omega)T_{qp}(j\omega) &\preceq (1-\epsilon)\gamma^{-2}I & \forall \omega \in \Omega \\ \implies \|T_{qp}\|_\infty^2 &\leq (1-\epsilon)\gamma^{-2} = \gamma_p^2 \end{aligned}$$

To show the equivalence with the result in [26], first apply row and column permutations to (23) to obtain

$$\begin{bmatrix} \gamma^{-2}I & G_{11}\Phi + G_{12}X & G_{11}\Psi & \vdots & 0 \\ * & \Phi^*\Phi & 0 & \vdots & \Phi^* \\ * & * & \Psi & \vdots & \Psi^* \\ \dots & \dots & \dots & \dots & \dots \\ 0 & \Phi & \Psi & \vdots & \epsilon^{-1}I \end{bmatrix} \succeq 0. \quad (40)$$

Since $\epsilon > 0$, the application of Schur's complement lemma yields

$$\begin{bmatrix} \gamma^{-2}I & G_{11}\Phi + G_{12}X & \vdots & G_{11}\Psi \\ (G_{11}\Phi + G_{12}X)^* & (1-\epsilon)\Phi^*\Phi & \vdots & 0 \\ \dots & \dots & \dots & \dots \\ (G_{11}\Psi)^* & 0 & \vdots & (1-\epsilon)\Psi \end{bmatrix} \succeq 0. \quad (41)$$

Let Ψ^g denote the generalised inverse of Ψ satisfying

$$\Psi\Psi^g\Psi = \Psi \quad \text{and} \quad (I - \Psi\Psi^g) \begin{bmatrix} (G_{11}\Psi)^* & 0 \end{bmatrix} = 0.$$

Note that $\Psi^g = \Psi$ satisfies these conditions, then using generalised Schur's complement lemma, [37, Theorem 1.20], we obtain:

$$\begin{bmatrix} \gamma^{-2}I - (1-\epsilon)^{-1}(G_{11}\Psi)(G_{11}\Psi)^* & G_{11}\Phi + G_{12}X \\ (G_{11}\Phi + G_{12}X)^* & (1-\epsilon)\Phi^*\Phi \end{bmatrix} \succeq 0.$$

Pre- and post-multiplication by $\begin{bmatrix} aI & 0 \\ 0 & I/a \end{bmatrix}$ where $a = \sqrt{1-\epsilon}$ gives,

$$\begin{bmatrix} (1-\epsilon)\gamma^{-2}I - (G_{11}\Psi)(G_{11}\Psi)^* & G_{11}\Phi + G_{12}X \\ (G_{11}\Phi + G_{12}X)^* & \Phi^*\Phi \end{bmatrix} \succeq 0.$$

Now choosing $\gamma_p^2 = (1-\epsilon)\gamma^{-2}$, the desired FDI (12) of [26] can be obtained.

$$\begin{bmatrix} \gamma_p^2 I - (G_{11}\Psi)(G_{11}\Psi)^* & G_{11}\Phi + G_{12}X \\ (G_{11}\Phi + G_{12}X)^* & \Phi^*\Phi \end{bmatrix} \succeq 0. \quad \square$$

REFERENCES

- [1] A. Megretski and A. Rantzer, "System analysis via integral quadratic constraints," *IEEE Transactions on Automatic Control*, vol. 42, no. 6, pp. 819–830, Jun. 1997.
- [2] J. Veenman and C. W. Scherer, "Stability analysis with integral quadratic constraints: A dissipativity based proof," in *52nd IEEE Conference on Decision and Control*, Dec. 2013, pp. 3770–3775.
- [3] P. Seiler, "Stability Analysis With Dissipation Inequalities and Integral Quadratic Constraints," *IEEE Transactions on Automatic Control*, vol. 60, no. 6, pp. 1704–1709, Jun. 2015.
- [4] M. Fetzer, C. W. Scherer, and J. Veenman, "Invariance With Dynamic Multipliers," *IEEE Transactions on Automatic Control*, vol. 63, no. 7, pp. 1929–1942, Jul. 2018.
- [5] M. Fu, S. Dasgupta, and Y. Chai Soh, "Integral quadratic constraint approach vs. multiplier approach," *Automatica*, vol. 41, no. 2, pp. 281–287, Feb. 2005.
- [6] J. Carrasco and P. Seiler, "Integral quadratic constraint theorem: A topological separation approach," in *2015 54th IEEE Conference on Decision and Control (CDC)*, Dec. 2015, pp. 5701–5706.
- [7] D. Hai-rong, G. Zhi-yong, W. Jin-zhi, and H. Lin, "Stability margin of systems with mixed uncertainties under the IQC descriptions," *Applied Mathematics and Mechanics*, vol. 23, no. 11, pp. 1274–1281, Nov. 2002.
- [8] H. Pfifer and P. Seiler, "Less conservative robustness analysis of linear parameter varying systems using integral quadratic constraints," *International Journal of Robust and Nonlinear Control*, vol. 26, no. 16, pp. 3580–3594, Nov. 2016.
- [9] J. Veenman, C. W. Scherer, and H. Koroğlu, "Robust stability and performance analysis based on integral quadratic constraints," *European Journal of Control*, vol. 31, pp. 1–32, Sep. 2016.
- [10] J. Veenman and C. W. Scherer, "IQC-Synthesis with General Dynamic Multipliers," *IFAC Proceedings Volumes*, vol. 44, no. 1, pp. 4600–4605, Jan. 2011.
- [11] J. Veenman, C. W. Scherer, C. Ardura, S. Bennani, V. Preda, and B. Girouart, "IQClab: A new IQC based toolbox for robustness analysis and control design," *IFAC-PapersOnLine*, vol. 54, no. 8, pp. 69–74, Jan. 2021.
- [12] S. Wang, H. Pfifer, and P. Seiler, "Robust synthesis for linear parameter varying systems using integral quadratic constraints," *Automatica*, vol. 68, pp. 111–118, Jun. 2016.
- [13] V. M. G. B. Cavalcanti and A. M. Simões, "IQC-synthesis under structural constraints," *International Journal of Robust and Nonlinear Control*, vol. 30, no. 13, pp. 4880–4905, Sep. 2020.
- [14] R. Pintelon and J. Schoukens, *System Identification: A Frequency Domain Approach*, 2nd ed. John Wiley & Sons, Ltd, 2012.
- [15] P. Apkarian and D. Noll, "Structured H_∞ -control of infinite-dimensional systems," *International Journal of Robust and Nonlinear Control*, vol. 28, no. 9, pp. 3212–3238, 2018.

-
- [16] M. Hast, K. Åström, B. Bernhardsson, and S. Boyd, "PID design by convex-concave optimization," in *2013 European Control Conference (ECC)*, Jul. 2013, pp. 4460–4465.
- [17] M. Saeki, "Data-driven loop-shaping design of PID controllers for stable plants," *International Journal of Adaptive Control and Signal Processing*, vol. 28, no. 12, pp. 1325–1340, 2014.
- [18] A. Karimi and G. Galdos, "Fixed-order H_∞ controller design for nonparametric models by convex optimization," *Automatica*, vol. 46, no. 8, pp. 1388–1394, Aug. 2010.
- [19] S. Boyd, M. Hast, and K. J. Åström, "MIMO PID tuning via iterated LMI restriction," *International Journal of Robust and Nonlinear Control*, vol. 26, no. 8, pp. 1718–1731, 2016.
- [20] A. Karimi, A. Nicoletti, and Y. Zhu, "Robust H_∞ controller design using frequency-domain data via convex optimization," *International Journal of Robust and Nonlinear Control*, vol. 28, no. 12, pp. 3766–3783, 2018.
- [21] A. Nicoletti and A. Karimi, "Robust control of systems with sector nonlinearities via convex optimization: A data-driven approach," *International Journal of Robust and Nonlinear Control*, vol. 29, no. 5, pp. 1361–1376, 2019.
- [22] T. Bloemers, T. Oomen, and R. Tóth, "Frequency Response Data-Based LPV Controller Synthesis Applied to a Control Moment Gyroscope," *IEEE Transactions on Control Systems Technology*, vol. 30, no. 6, pp. 2734–2742, Nov. 2022.
- [23] A. Karimi and C. Kammer, "A data-driven approach to robust control of multivariable systems by convex optimization," *Automatica*, vol. 85, pp. 227–233, Nov. 2017.
- [24] S. S. Madani, C. Kammer, and A. Karimi, "Data-Driven Distributed Combined Primary and Secondary Control in Microgrids," *IEEE Transactions on Control Systems Technology*, vol. 29, no. 3, pp. 1340–1347, May 2021.
- [25] S. S. Madani and A. Karimi, "Data-Driven Passivity-Based Current Controller Design for Power-Electronic Converters of Traction Systems," in *Proceedings of the IEEE Conference on Decision and Control*, Jeju Island, Republic of Korea, Dec. 2020, pp. 842–847.
- [26] P. Schuchert, V. Gupta, and A. Karimi, "Data-driven fixed-structure frequency-based H_2 and H_∞ controller design," *Automatica*, vol. 160, p. 111398, Feb. 2024.
- [27] A. Koch, J. Berberich, J. Köhler, and F. Allgöwer, "Determining optimal input–output properties: A data-driven approach," *Automatica*, vol. 134, p. 109906, Dec. 2021.
- [28] T. Bloemers, T. Oomen, and R. Toth, "Frequency Response Data-Driven LPV Controller Synthesis for MIMO Systems," *IEEE Control Systems Letters*, vol. 6, pp. 2264–2269, 2022.
- [29] K. Zhou, J. C. Doyle, and K. Glover, *Robust and Optimal Control*. New Jersey, USA: Prentice Hall, 1996.
- [30] D. S. Bernstein, *Matrix Mathematics: Theory, Facts, and Formulas*, 2nd ed. Princeton University Press, Jul. 2009.
- [31] S. Skogestad and I. Postlethwaite, *Multivariable Feedback Control: Analysis and Design*. West Sussex: John Wiley & Sons Ltd., 1996.
- [32] G. Calafiore and M. Campi, "The Scenario Approach to Robust Control Design," *IEEE Transactions on Automatic Control*, vol. 51, no. 5, pp. 742–753, May 2006.
- [33] J. Veenman and C. W. Scherer, "IQC-synthesis with general dynamic multipliers," *International Journal of Robust and Nonlinear Control*, vol. 24, no. 17, pp. 3027–3056, 2014.
- [34] C.-Y. Kao and A. Rantzer, "Stability analysis of systems with uncertain time-varying delays," *Automatica*, vol. 43, no. 6, pp. 959–970, Jun. 2007.
- [35] V. Gupta, E. Klauser, and A. Karimi, "Data-driven IQC-based robust control design for hybrid micro-disturbance isolation platform," in *2023 IEEE Conference on Decision and Control (CDC)*, Dec. 2023.
- [36] E. Onillon, T. Adam, G. B. Gallego, and E. Klauser, "CSEM micro-vibration characterisation facility description and validation," in *19th European Space Mechanisms and Tribology Symposium (ESMAT) 2021*, Sep. 2021.
- [37] F. Zhang, Ed., *The Schur Complement and Its Applications*, ser. Numerical Methods and Algorithms. New York: Springer-Verlag, 2005, vol. 4.